Energetics, bonding mechanism, and electronic structure of metal-ceramic interfaces: Ag/MgO(001)

Chun Li, Ruqian Wu, and A. J. Freeman
Department of Physics and Astronomy, Northwestern University, Evanston, Illinois 60208

C. L. Fu
Metals and Ceramics Division, Oak Ridge National Laboratory, Oak Ridge, Tennessee 37831
(Received 22 March 1993)

Electronic-structure total-energy investigations for the metal-ceramic interface system Ag/MgO(001) show that the preferred adsorption site for the overlayer Ag atom is above the O site of the clean MgO(001) surface. The binding energy of the overlayer Ag atom on the MgO(001) surface is 0.3 eV/atom (0.64 J/m^2). No significant charge transfer is found between the overlayer Ag and the MgO(001) substrate, and the interface effect on the MgO(001) substrate is limited to the interface layer. The Ag overlayer shows typical metal features in the electronic band structure as well as in the charge distributions. The interface O atom is slightly metallized, i.e., the occupied states at the Fermi energy have hybridized O-Ag character. Compared with the O, the Mg is less influenced by the Ag.

I. INTRODUCTION

Metal-ceramic interfacial properties have attracted considerable attention in recent years due to their technological applications such as structural, electronic, chemical catalysis, high temperature, etc.[1] Among them, interfaces with magnesium oxide (MgO) as a substrate are among the most frequently studied.

Experimentally, the electronic structure of the MgO(100) clean surface was studied by Henrich, Dresselhaus, and Zeiger[2] using energy-dependent electron-energy-loss spectroscopy (EELS). The surface-state structure seen in O-to-Mg loss spectra agrees with discrete variational $X\alpha$ calculations of the MgO(100) surface.[3] For the interfaces between noble metals (Cu, Au) and MgO, Fecht and Gleiter[4] found that the most preferred orientation relationships between the noble metal and MgO are $\langle 100\rangle_{\text{metal}}/\langle 100\rangle_{\text{MgO}}$ and $\langle 110\rangle_{\text{metal}}/\langle 110\rangle_{\text{MgO}}$, i.e., the orientation with the highest symmetry (referred to as a "lock-in" model). Fuchs, Treilleux, and Thevenard[5] investigated thin films of Ag deposited on MgO single crystals or multilayers (Ag-MgO or MgO-Ag-MgO) grown on NaCl or KBr single crystals. They found that Ag thin films are grown epitaxially on the MgO(100) surface, and that Xe irradiation induces significant interdiffusion at the Ag-MgO interface. Hoel[6] also reported epitaxially grown Au thin films on the MgO(001) surface.

Results of transmission electron microscopy determinations of the interface structure are consistent with the "lock-in" model. Ou and Cowley[7] applied scanning reflection electron microscopy techniques to the interfaces of Cu (and Pd) on MgO(001). The as-deposited Cu particles tend to align along [100]. He and Möller[8] reported a series of experimental studies of ultrathin Cu films on MgO(100) and MgO(111) substrates prepared by electron-beam evaporation techniques. Structural and electronic studies using low-energy electron diffraction (LEED), Auger electron spectroscopy (AES), EELS, etc., concluded that Cu grows epitaxially on MgO(001); that the electronic changes of MgO are induced in the first layer by the deposition of Cu; that initially deposited Cu atoms (well below one monolayer coverage) exist in an ionized state and are bonded to the oxygen ions; and that further deposition of Cu gives rise to the formation of a mixed monolayer of nonmetallic and metallic Cu. As determined by Delplancke *et al.*,[9] both Cu and Rh thin films grow expitaxially on a MgO(100) substrate, and the latter is found to have good thermal stability at high temperatures for expitaxy. Significantly, it was found that the adhesion M/MgO interfaces correlates with the corresponding formation free energy for metal (M) oxide (both increase in the order M=Ag, Cu, Ni, Fe, etc.).[10] This implies that somewhat covalent p-d bonds may exist between M-O, although it has been established that the M/MgO interfaces are atomically sharp without interdiffusion and formation of the M-oxide layer.

On the other hand, theoretical calculations for the surface electronic structure of MgO(100) have been reported by a few groups. Lee and Wong[11] used Green's-function and linear combination of atomic orbitals (LCAO) calculations to study the surface band structure of MgO. They found that there are surface states of MgO(001) lying about 0.5 eV above the bulk O 2p band. $X\alpha$ cluster calculations for the MgO surface by Satako, Tsukada, and Adachi[3] found that a peak in the surface density of states occurs 2 eV below the bottom of the bulk Mg 3s conduction band. Schönberger, Andersen, and Methfessel[12] carried out full-potential linearized muffin-tin orbital (FLMTO) calculations for Ti/MgO(001) and Ag/MgO(001) interfaces in a superlattice geometry, and found that both Ti and Ag bind on top of oxygen and that the interface force constants for Ti/MgO(001) are 3–4 times larger than that for Ag/MgO(001). By consid-

ering the Coulomb interaction between ceramics and their images in the metal layer (long-wavelength charge fluctuations only), Duffy, Arding, and Stoneham[13] found that the metal-ceramic interface is stabilized by the balance between the electrostatic attraction and the interatomic hard-core repulsion. Furthermore, thermodynamic properties of the MgO surface have also been studied by a few groups.[14]

Very recently, we carried out full-potential linearized augmented-plane-wave (FLAPW) calculations for Fe/MgO(001).[15] Surprisingly, the magnetic moment for the Fe overlayer is as large as $3.1\mu_B$ (almost the same as that for a free standing Fe monolayer) due to the lack of overlayer-substrate interaction. Thus it offers an ideal system to study two-dimensional (2D) magnetism, although to synthesize a high quality Fe monolayer on MgO(001) still remains a tremendous challenge for experimentalists.[16]

In this work, we investigated the Ag/MgO(00) system to study the metal-ceramic interface using the FLAPW method. As is well known, pure MgO has a NaCl crystal structure, one of the most convenient for model calculations. The (001) surface is by far the most stable surface of most alkaline-earth oxides, which is almost an unrelaxed termination of the bulk lattice.[1] Ag has simple metal features and is rather predictable in its behavior when interfaced with other materials. Also, the short range of the surface-interface effects for noble metals (less than one atomic layer)[17] provides a sound basis for emphasizing the real metal-ceramic interface by including only a small number of Ag layers in the model calculations. The not-too-large lattice mismatch between the MgO(001) and fcc Ag(001) surfaces (4%) is a necessary condition for a simple structure low-energy interface between these two materials.

Following a brief description of the methodology and computational models, we present in later sections our first-principles electron band-structure results for bulk MgO, the clean MgO(001) surface, and the Ag/MgO(001) interface.

II. METHODOLOGY AND COMPUTATIONAL MODELS

We employed the FLAPW method[18] to study the structural properties and electronic structure of (i) bulk MgO, (ii) the clean MgO(001) surface, (iii) a free standing Ag monolayer, and (iv) an Ag monolayer adsorbed on the MgO(001) surface with Ag atoms located either above the O, the Mg, or the hollow site. In all the calculations, the muffin-tin (MT) radius of Mg and O was set at 1.70 a.u., and that of Ag was set at 2.20 a.u. The Mg $1s$ and $2s$, O $1s$, and Ag $1s$, $2s$, $2p$, $3s$, $3p$, $3d$, $4s$, and $4p$ electrons were treated as core electrons, and all the others were treated as valence electrons.

In the FLAPW method, no shape approximation is made for either the potential or charge densities. The core electrons are treated relativistically, and the valence electrons are treated semirelativistically, i.e., no spin-orbit interaction is included in the Hamiltonian. Plane waves (PW's) with an energy cutoff of 12.5 Ry (corresponding to 1000 PW's for Ag/MgO) were used to represent the electronic wave functions. Spherical harmonics with angular momentum up to $l=8$ were used to express the charge density and potential inside the MT sphere. We used 21 uniformly distributed k points in the $\frac{1}{8}$ irreducible 2D Brillouin zone (BZ). The Kohn-Sham equations were solved self-consistently, and convergence was assumed when the difference between the input and output charge densities is smaller than 10^{-4} electrons/(a.u.).[3]

III. RESULTS AND DISCUSSION

A. Bulk MgO

As a first step, we calculated the structural and electronic properties of bulk MgO using the bulk FLAPW method. The total energy calculated versus volume yielded the optimized lattice constant 4.247 Å, which is about 1% larger than the experimentally measured lattice constant 4.205 Å. This result provides evidence that local-density approximation (LDA) calculations can be used to describe ionic systems (especially for ground-state properties). The lowest excited (Mg) states lie about 5 eV above the top of the valence band—a value about 40% smaller than the measured band gap. This difference however, is expected from the lack of core hole relaxation in the local-density description of the excitation.

B. Clean MgO(001) surface

The clean MgO(001) surface is represented by a single slab of five atomic layers of MgO in the NaCl structure. We used the experimental lattice constant $a=4.205$ Å throughout the following calculations. Since MgO(001) is almost an unrelaxed termination of the bulk, no surface reconstruction or relaxation was considered. The charge density of the single slab in the (100) plane is shown in Fig. 1(a). The charge corrugation is very weak on MgO(001), since the outermost contours are very smooth. The surface effects are largely limited to the upper half of the surface layer, and the charge-density contours of the nonsurface atoms are consistently bulklike in shape. This is also seen in the list of the charge populations inside the MT spheres given in Table I. The surface O charge population is smaller than that of bulklike O by about 0.05 electrons, and the surface Mg charge population is smaller than that of bulklike Mg by 0.01 electrons—a result of electron spilling from O and Mg atoms into the vacuum region.

To get an insight into the formation of the MgO crystal and surface, charge-density difference contours between the self-consistent and atomic superimposed charge densities are plotted in Fig. 1(b). As expected, oxygen atoms gain electrons from Mg sites and even from the interstitial region to form a complete $2p$ shell. In the bulk region, contours around O are highly spherically symmetric—indicating the ionic character of the Mg-O interaction. It is obvious that the charge accumulations in the top-half surface O sites are smaller than in the

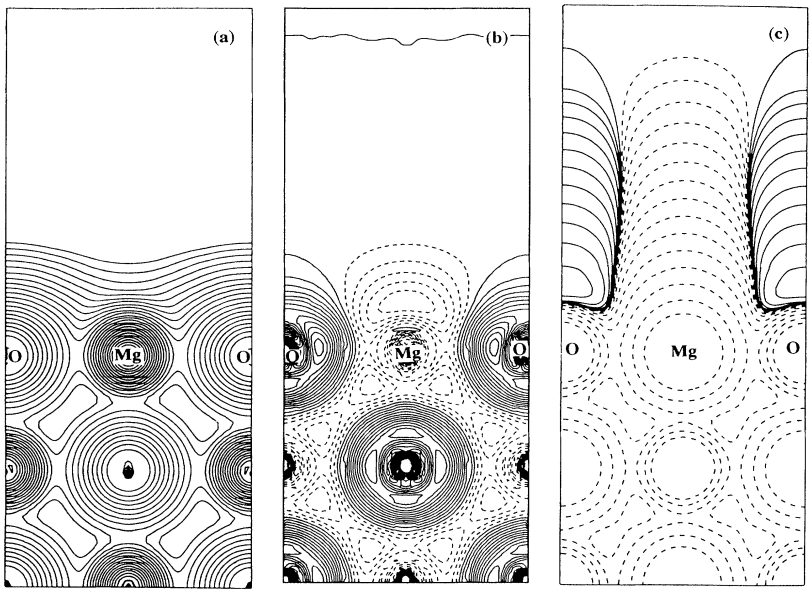

FIG. 1. (a) The charge-density distribution for the clean MgO(001) five-layer slab plotted for the upper half of a single slab unit cell in the (100) plane; contours start from 1×10^{-3} e/a.u.^{3} and increase successively by a factor of $\sqrt{2}$. (b) The charge-density difference between the self-consistent and the atomic superimposed charge densities; successive contours start from 0 (the first solid line), with an increment of $\pm2\times10^{-3}$ e/a.u.^{3} (c) The effective Coulomb potential for the clean MgO(001) slab; contours start from $\pm10^{-4}$ a.u., change successively and by a factor of 2. Solid (dashed) lines indicate positive (negative) values.

bottom-half region—which suggests that the ionic MgO interaction is somewhat weakened in the surface region.

In Fig. 1(c), the Coulomb potential (V_c) calculated for the clean MgO(001) surface is shown. For both the Mg and O atoms, the potential also shows good spherical symmetry within their atomic radii (i.e., touching MT radii); obviously due to the strong charge transfer from the Mg to O sites, the electronstatic potential around Mg atoms is more negative than that at O sites. It is interesting to note that at the surface, the potential has positive values (repulsive) in regions above the surface O, and negative values (attractive) above Mg, and a sharp boundary is seen between the positive and negative potential regions. However, since the charge density on top of the oxygen atoms is much larger than that over Mg atoms, the total potential, i.e., $V=V_c+V_{xc}$, is very smooth in the vacuum region.

The layer-projected density of states (DOS) of MgO(001) plotted in Fig. 2 shows that the DOS in the Mg MT spheres (tail of O states) is much smaller in value compared with that of the O atoms for the occupied states. As for charge densities, the DOS also converges to being bulklike from the second layer (indicated by the similarity between the DOS curves of the second and the center layers). Due to the weakened surface ionic Mg-O interaction, the surface band gap is 1.5 eV smaller than

TABLE I. Charge population of the calculated systems, projected by l values and atoms.

	MgO five-layer clean surface					
		Mg			O	
layer	3s	2p	total	2s	2p	total
center	0.077	5.850	6.067	1.634	3.851	5.489
S-1	0.078	5.850	6.069	1.634	3.851	5.490
surface	0.075	5.859	6.057	1.635	3.802	5.440
	Ag above the O site					
		Mg			O	
center	0.076	5.848	6.065	1.635	3.847	5.486
I-1	0.077	5.848	6.066	1.636	3.846	5.486
interface	0.073	5.851	6.047	1.642	3.782	5.429
	Ag in Ag/MgO					
5s		5p		4d		total
0.237		0.055		8.657		8.953
	Free-standing Ag monolayer					
0.240		0.040		8.652		8.936

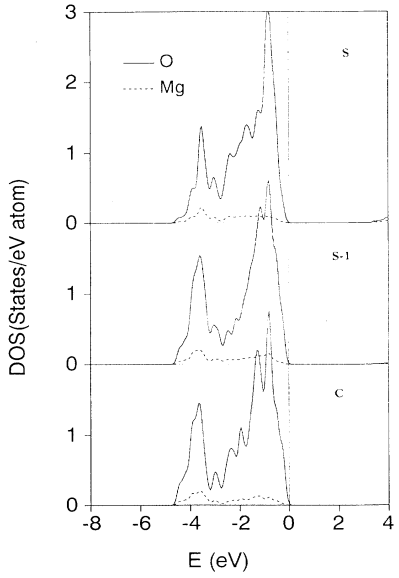

FIG. 2. The layer-projected density of states (DOS) of the conduction electrons in units of states/eV atom for the clean MgO(001) surface.

that obtained for bulk layers, even though the lowest Mg states are still 3.5 eV higher than in energy oxygen states. Combining this with the fact that Ag d states lie well below E_F, the Mg-Ag interaction should be much weaker than the O-Ag interaction.

C. Ag/MgO(001)

1. Site preference of Ag on MgO

The metal-ceramic interface between Ag and MgO is represented by a monolayer of Ag adsorbed on the surfaces of the MgO(001) slab. Three possible adsorption sites of Ag atoms on the MgO(001) surface, i.e., above the O atom, above the Mg atom, or in the hollow site, are considered in the calculations. The total energy vs interlayer spacing of these three possible positions of a Ag overlayer on the MgO(001) surface, plotted in Fig. 3, shows that for Ag the site above O is preferred over the others. This is somewhat expected since Ag atoms have more chance to interact with O $2p$ states (Ag d–O p), considering that Mg states lie 3–5 eV above E_F. In fact, as shown in Fig. 3, the Ag-O interaction may reduce the total energy considerably compared to the case with Ag on the Mg sites, especially for shorter interatomic distances. The optimized interlayer spacing between the Ag monolayer and the MgO surface layer is 5.1 a.u. (2.70 Å) for Ag above the O site. This value is about 7% larger than that obtained in FLMTO calculations for the Ag/MgO(001) interface in a superlattice,[11] where the interfacial Ag layer is pushed by other Ag layers from above. In the following discussions, the properties of the Ag/MgO(001) system are obtained with our optimized interlayer spacing.

It is interesting to note that model calculations of an isolated noble-metal atom (Au) on the surface of alkali halides (NaCl, NaF, KCl, and KBr) by Buckingham, and Robins[19] showed that the metal atoms tend toward the sites above the positive ions (Na and K). A similar result was also concluded for Ag atoms on NaCl(001),[20] using van der Waals adhesion model calculations. However, the semiempirical image charge[14] results in Ag being above the hole sites. In contrast, our results indicate that the Ag monolayer tends toward the site above the (negative) O atom. The difference however, is, due to the fact that MgO is a weaker ionic crystal compared to alkali halides, so that some chemical interactions (although not strong) may be involved in the Ag/MgO adsorption process. Experimental measurements for the adsorption sites are highly desired to verify these theoretical results, since they may help to define the main mechanism at the Ag/MgO interface.

2. Charge density

Since the charge density is the fundamental feature of density-functional theory, a plot of the charge-density contours in the (100) plane of the Ag/MgO system is shown in Fig. 4. Its charge population is listed in Table I. Compared with the clean MgO five-layer slab, the electron populations at Mg and O in the center and the subinterface (I-1) layers remain essentially unchanged. In the interface layer, both Mg and O atoms show a net decrease of the total charge on the order of 0.01 electrons in comparison with the surface layer of the clean MgO five-layer slab. This net decrease is caused by the loss of Mg $3p$ electrons and O $2p$ electrons.

Compared with the charge population of the free Ag monolayer, the charge population of the Ag atom in the

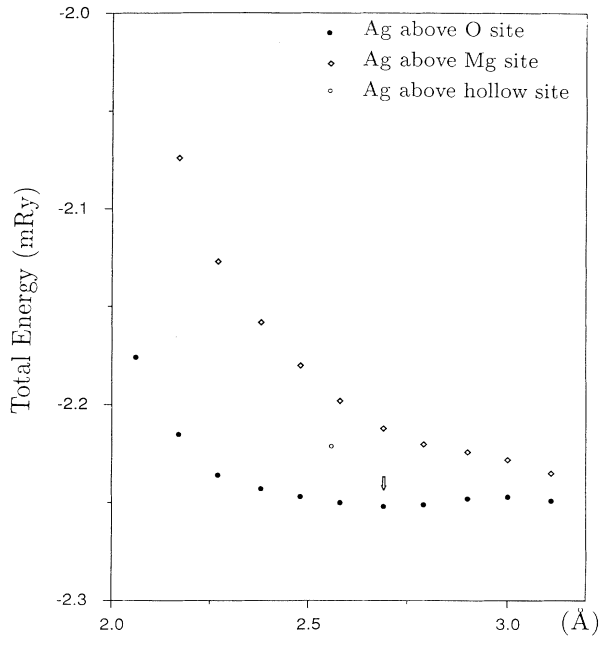

FIG. 3. The total energy vs interlayer spacing for three possible positions of Ag overlayer atoms on the MgO(001) surface: Ag above the O site; Ag above the Mg site; and Ag above the hollow site.

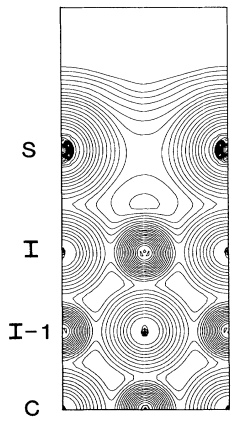

FIG. 4. The charge-density distribution for the Ag/MgO(001) (Ag above the O site) slab plotted for the upper half of a single slab unit cell in the (100) plane. Contours start from 1×10^{-3} e/a.u.,^{3} and increase successively by a factor of $\sqrt{2}$.

Ag/MgO system is only slightly larger (by ~ 0.02 electrons), indicating no significant charge transfer.

At the Fermi level, the energy-sliced charge density provides information about the nature of these important mobile conduction electrons. As seen from Fig. 5, the majority of these are from the Ag layer; however, interfacial O atoms also contribute. This shows that the overlayer Ag atoms form a one-layer conductor, and that the interface O atoms are slightly metallized. Interestingly, the Mg atoms do not share any of the conduction electrons, and thus are not metallized.

3. *Band structure*

The conduction-electron band structure of Ag/MgO (with Ag above the O site) is shown in Fig. 6. The solid lines denote localized surface states whose wave functions have more than 50% weight within the overlayer Ag atom. The Ag $4d$ and O $2p$ bands are very close in energy and show significant hybridization. The only band crossing the Fermi level is the hybridized Ag s-p and O s-p electron band; it crosses E_F at two points along the high-symmetry directions, i.e., $\sim 1/5$ from $\bar{X}$ toward $\bar{\Gamma}$ along $\bar{\Delta}$, and $\sim 3/5$ from $\bar{\Gamma}$ toward $\bar{M}$ along $\bar{\Sigma}$. The top of the O $2p$ and Ag $4d$ band is located at $\bar{\Gamma}$ with energy -2 eV below E_F. The bottom of the empty O $3s$ band is also located at $\bar{\Gamma}$, with an energy $+1.5$ eV above E_F.

4. *Density of states*

The layer-projected partial DOS of the conduction electrons of Ag/MgO(001) is shown in Fig. 7. The overlayer Ag DOS has the shape typical for a Ag-metal monolayer, with the Ag $4d$ states in the energy range -5 to -2 eV below E_F. The electron states with energy close to E_F are primarily from Ag s- and p-like electrons. The noninterface O atoms remain insulating, because of the lack of electron states at the Fermi level. The interface O DOS is evidently different from that seen for the noninterface O atoms, i.e., a narrower width for the main peak and an extended tail from s-p electron states crossing E_F—a result of the interfacial hybridization with Ag atoms.

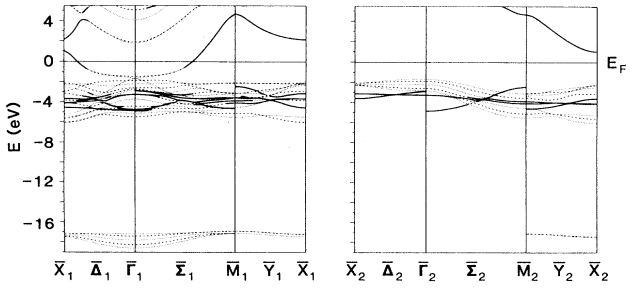

FIG. 6. Energy bands along high-symmetry directions in the 2D Brillouin zone for the Ag/MgO(001) (Ag above the O site) single lab. Symmetry points subscripted by 1 and 2 denote even and odd reflection symmetries, respectively. Dashed and dotted lines represent even and odd parities with respect to the z reflection. Solid lines indicate states whose wave function has more than 50% weight within the overlayer Ag atom.

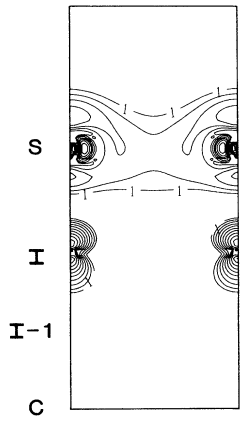

FIG. 5. The energy-sliced charge density at the Fermi level for Ag/MgO(001) (Ag above the O site). Contours start from 1×10^{-3} e/a.u.^{3} and increase successively by a factor of $\sqrt{2}$.

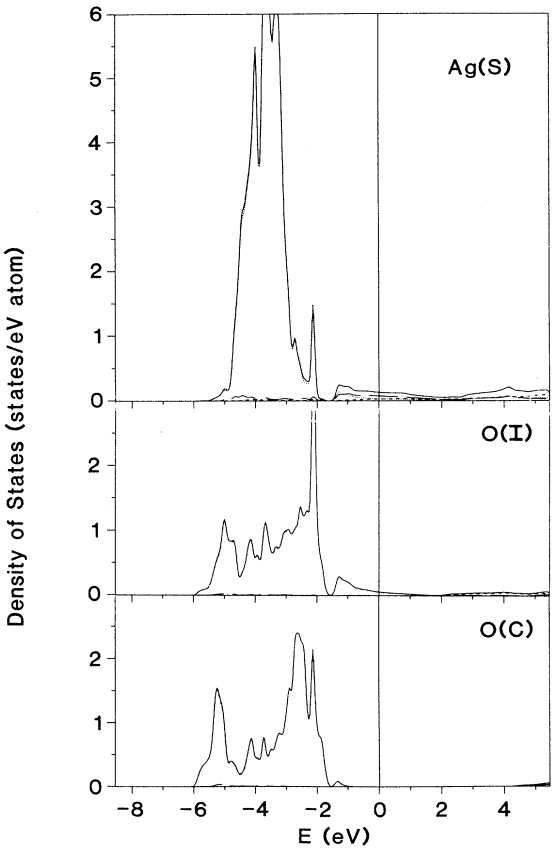

FIG. 7. The layer-projected density of states (DOS) of the conduction electrons in units of states/eV atom for Ag/MgO(001) (Ag above the O site).

D. Ag Binding Energy

By comparing the total energies of the systems calculated, i.e., Ag/MgO, the MgO(001) clean surface, and the unsupported Ag monolayer, we obtain the binding energy of Ag atoms on a clear MgO surface as 0.3 eV/atom (0.64 J/m^2). This adsorption energy indicates that Ag/MgO(001) belongs to a physisorption class ($E_b < 0.5$ eV/atom) instead of chemisorption ($E_b > 0.5$ eV/atom). Such a result is expected, since, as discussed Sec. III C, there is no noticeable charge transfer and chemical bonding exists in this system. Combined with the fact that the energy differs only slightly for different adsorption sites (< 2 meV/atom), MgO appears very flat and seems to lack stickiness for adsorbates. This is the reason why it is hard to grow high quality metallic overlayers (e.g., Fe) on MgO.[13]

ACKNOWLEDGMENTS

Work at Northwestern University was supported by the U.S. Department of Energy (Grant No. DE-FG02-88ER45372) and by a grant of computing time on the BES CRAY supercomputer at NERSC, LLNL. Work at Oak Ridge National Laboratory sponsored by the Division of Material Sciences, U.S. Department of Energy, under Contract No. DE-AC05-84OR21400 with Martin Marietta Energy Systems, Inc.

[1]V. E. Henrich, Rep. Prog. Phys. **48**, 1481 (1985); D. R. Clarke and D. Wolf, Mater. Sci. Eng. **83**, 197 (1986); A. P. Sutton and R. W. Balluffi, Acta. Metall. **35**, 2177 (1987); R. W. Balluffi, M. Rühle and A. P. Sutton, Mater. Sci. Eng. **89**, 1 (1987).

[2]V. E. Henrich, G. Dresselhaus, and H. J. Zeiger, Phys. Rev. B **22**, 4764 (1980).

[3]C. Satako, M. Tsukada, and H. Adachi, J. Phys. Soc. Jpn. **45**, 1333 (1978).

[4]H. J. Fecht and H. Gleiter, Acta Metall. **33**, 557 (1985); H. J. Fecht, *ibid.* **36**, 689 (1988).

[5]G. Fuchs, M. Treilleux, and P. Thevenard, Thin Solid Films **165**, 347 (1988).

[6]R. H. Hoel, Surf. Sci. **169**, 317 (1986).

[7]H.-J. Ou and J. M. Cowley, Ultramicroscopy **22**, 207 (1987).

[8]Jain-Wei He and P. J. Möller, Surf. Sci. **180**, 411 (1987); **178**, 934 (1986); I. Alstrup and P. J. Möller, Appl. Surf. Sci. **33/34**, 143 (1988).

[9]M. P. Delplancke, P. Delcambe, L. Binst, M. Jardinier-Offergeld, and F. Bouillon, Thin Solid Films **143**, 43 (1986).

[10]K. H. Johnson and S. V. Pepper, J. Appl. Phys. **53**, 6634 (1982).

[11]V. C. Lee and H. S. Wong, J. Phys. Soc. Jpn. **45**, 895 (1978).

[12]U. Schönberger, O. K. Andersen, and M. Methfessel, Acta Metall. Mater. **40**, 51 (1992).

[13]D. M. Duffy, J. H. Arding, and A. M. Stoneham, Acta Metall. Mater. **40**, 511 (1992).

[14]T. S. Chen, F. W. de Wette, and A. P. Alldredge, Phys. Rev. B **15**, 1167 (1977); R. N. Barnett and R. Bass, *ibid.* **19**, 4259 (1979); G. Lakshmi and F. W. de Wette, *ibid.* **22**, 5009 (1980); **23**, 2035 (1981).

[15]Chun Li and A. J. Freeman, Phys. Rev. B **43**, 780 (1991).

[16]T. Urano and T. Kanaji, J. Phys. Soc. Jpn. **57**, 3043 (1988); Y. Y. Huang, C. Liu, and G. P. Felcher, Phys. Rev. B **47**, 183 (1993).

[17]H. Erschbaumer, A. J. Freeman, C. L. Fu, and R. Podloucky, Surf. Sci. **243**, 317 (1991).

[18]E. Wimmer, H. Krakauer, M. Weinert, and A. J. Freeman, Phys. Rev. B **24**, 864 (1981), and references therein.

[19]E. M. Chan, M. J. Buckingham, and J. L. Robins, Surf. Sci. **67**, 285 (1977).

[20]H. von Harrach, Thin Solid Films **22**, 305 (1974).